Aalborg Universitet

AALBORG UNIVERSITY
DENMARK

Progressive Damage Simulation of Laminates in Wind Turbine Blades under Quasistatic and Cyclic Loading.

Bak, Brian Lau Verndal

PROGRESSIVE DAMAGE SIMULATION OF LAMINATES IN WIND TURBINE BLADES UNDER QUASISTATIC AND CYCLIC LOADING

BY
BRIAN LAU VERNDAL BAK

DISSERTATION SUBMITTED 2015

AALBORG UNIVERSITY
DENMARK

PROGRESSIVE DAMAGE SIMULATION OF LAMINATES IN WIND TURBINE BLADES UNDER QUASISTATIC AND CYCLIC LOADING

BY
BRIAN LAU VERNDAL BAK

AALBORG UNIVERSITY
DENMARK

Preface

This thesis has been submitted to the Faculty of Engineering and Science at Aalborg University in partial fulfillment of the requirements for the degree of Doctor of Philosophy in Mechanical Engineering. The thesis is written as a collection of peer-reviewed papers in the format recommended by the Doctoral School of Engineering and Science. The Ph.D. project is a part of the industrial Ph.D. project programme and is a collaboration between Siemens Wind Power A/S and Aalborg Universty. The Ph.D. project is a part of the research project Danish Centre for Composite Structures and Materials for Wind Turbines (DCCSM, grant no. 09-067212 from the Danish Council for Strategic Research) of which one of the main focus areas of is computational methods for cracks and damage on length scales from nanometer to decameter scale of laminated composite structures.

Aalborg, March 2015

Brian Bak

Abstract

The overall purpose of this Ph.D. thesis is to develop a framework of methods for progressive delamination modeling and simulation of composite laminates in large scale structures under both quasi-static and fatigue loading. The purpose is motivated by a wish to reduce the cost and consumption of materials while ensuring high a quality of wind turbine blades.

The first part of the thesis is an introduction to the project and provides a short introduction to selected basic topics of the theoretical background of the presented papers. The in-depth state-of-the-art review is provided in the papers. The second part of the thesis consists of three refereed journal papers.

Paper A is concerned with computational efficiency, ability to converge to a solution and accuracy of the solution when large cohesive elements are applied to quasi-static delamination analyses. It is shown that the accuracy and computational efficiency are improved by reducing the integration error introduced by the numerical integration of the element force vector and stiffness matrix. Paper B presents a review of the available experimental observations, the phenomenological models and the computational simulation methods for the three phases of fatigue-driven delamination (initiation, onset and propagation). The review clarifies which capabilities are required from simulation methods and next review these simulation methods in regards to these capabilities. The overall procedure and characteristics of the methods are described. Paper C presents a new method for simulating fatigue-driven delamination under general mixed mode conditions. The method is capable of simulating both quasi-static and fatigue crack propagation and depend only on easily obtainable material parameters. The experimentally obtained crack growth rate can be reproduced in finite element analyses with practically no error for any given structure and load.

Dansk Resumé

Det overordnede formål med denne Ph.D. afhandling er at udvikle et sæt af metoder til modellering, simulering og analyse af delamineringspropagering i laminerede kompositmaterialer brugt i store strukturer under både kvasi-statiske laster og udmattelse. Dette formål er motiveret af et ønske om at reducere materialeomkostningerne for vindmøllevinger, mens der samtidig sikres en høj kvalitet.

Første del af afhandlingen er en introduktion til projektet og giver en kort indføring i udvalgte basale emner indenfor den anvendte teori i de udarbejdede tidsskriftartikler. Den anden del af afhandlingen består af tre videnskabelige tidskriftsartikler, indeholdende dybdegående redegørelse for state-of-the-art.

Artikel A handler om den beregningsmæssige effektivitet, evnen til at konvergere til en løsning og nøjagtigheden af den fundne løsning, når store kohæsive elementer bruges i kvasi-statiske delamineringsanalyser. Det vises, at nøjagtigheden og den beregningsmæssige effektivitet forbedres ved at reducere den integrationsfejl, der introduceres i forbindelse med den numeriske integration af elementkraftvektoren og elementstivhedsmatricen. Artikel B præsenterer en udredning af de tilgængelige eksperimentelle observationer samt de phenomenologiske modeller og simuleringsmetoder for de tre faser af udmattelsesdrevne delamineringer (initiering, "onset" og propagering). Udredningen klargør, hvilke egenskaber der er nødvendige for simuleringsmetoderne at besidde, og gør desuden rede for hver enkelt metode i forhold til disse egenskaber. Metodernes overordnede fremgangsmåde og karakteristika er beskrevet. Paper C præsenterer en ny metode til at simulere udmattelsesdrevne delamineringer under generelle mixed mode betingelser. Metoden kan simulere revnevækst under både kvasi-statiske laster og udmattelse, og afhænger kun af let tilgængelige materialeparametre. Den eksperimentelt bestemte revnevæksthastighed kan blive genskabt i finite element analyser med praktisk talt ingen fejl.

Thesis Details

This thesis is made as a collection of papers and consists of an introduction to the area of research and three papers for publication in refereed scientific journals of which two are accepted and one is submitted in revised form.

Thesis Title:	Progressive Damage Simulation of Laminates in Wind Turbine Blades under Quasi-static and Cyclic Loading
Ph.D. Student:	Brian L. V. Bak
Ph.D. Supervisors:	Erik Lund, Prof., Ph.D., M.Sc. Department of Mechanical and Manufacturing Engineering, Aalborg University, Denmark
	Esben Lindgaard, Assoc. Prof., Ph.D., M.Sc. Department of Mechanical and Manufacturing Engineering, Aalborg University, Denmark
Company supervisor:	Christian Frier Hvejsel, Team Lead, Ph.D., M.Sc. Blade Design department, Siemens Wind Power A/S, Denmark
3rd Party supervisors:	Albert Turon, Assoc. Prof., Ph.D., M.Sc. AMADE, Polytechnic School, University of Girona, Spain
	Bent F. Sørensen, Program leader, Ph.D. Risø DTU, Materials Research Division, Technical University of Denmark

Publications in refereed journals

A) Bak, B.L.V., Lindgaard, E., Lund, E. 2014. Analysis of the Integration of Cohesive Elements in regard to Utilization of Coarse Mesh in Laminated Composite Materials, *International Journal for Numerical Methods in Engineering*, **99**(8), pp. 566–586.

B) Bak, B.L.V., Sarrado, C., Turon, A., and Costa, J., 2014. Delamination under Fatigue Loads in Composite Laminates: A Review on the Observed Phe-

nomenology and Computational Methods, *Applied Mechanics Reviews*, **66**(6), pp. 1–24.

C) Bak, B.L.V., Turon, A., Lindgaard, E., Lund, E., 2014. A Simulation Method for High-Cycle Fatigue-Driven Delamination using a Cohesive Zone Model, submitted to: *International Journal for Numerical Methods in Engineering*.

Publications in proceedings with review

D) Bak, B.L.V.; Lindgaard, E.; Lund, E.; Turon, A. (2014): "Performance of Cohesive Zone Models for High-Cycle Fatique Driven Delaminations". *In: Proc. of 11th World Congress on Computational Mechanics (WCCM XI), 5th European Conference on Computational Mechanics (ECCM V), 6th European Conference on Computational Fluid Dynamics (ECFDVI)* (eds. E. Onate, X. Oliver, A. Huerta), 20 - 25 July, 2014, 2 pages.

E) Bak, B.; Lund, E. (2012): "Utilization of Large Cohesive Interface Elements for Delamination Simulation". *In: Proc. ECCM15- 15Th European Conference On Composite Materials*, Venice, Italy, 24-28 June 2012, 8 pages, ISBN 978-88-88785-33-2.

F) Bak, B.; Lund, E. (2011): "Reducing the Integration Error of Cohesive Elements". *In: Proc. 24th Nordic Seminar on Computational Mechanics, NSCM24* (eds. J. Freund and R. Kouhia), 3-4 November, 2011, Helsinki, Finland, Aalto University, School of Engineering, Department of Civil and Structural Engineering, pp. 85–88, ISBN 978-952-60-4347-0, ISSN 1799-4896.

This thesis has been submitted for assessment in partial fulfillment of the PhD degree. The thesis is based on the submitted or published scientific papers which are listed above. Parts of the papers are used directly or indirectly in the extended summary of the thesis. As part of the assessment, co-author statements have been made available to the assessment committee and are also available at the Faculty. The thesis is not in its present form acceptable for open publication but only in limited and closed circulation as copyright may not be ensured.

Contents

Chapter 1

Introduction to the Ph.D. project

The presented work is conducted as an industrial Ph.D. project for Siemens Wind Power A/S (SWP) as a part of the research project Danish Centre for Composite Structures and Materials for Wind Turbines (DCCSM, grant no. 09-067212 from the Danish Council for Strategic Research). The work was initiated by the wish of SWP to expand the current set of strength based computational design analysis and verification tools with computational simulation tools for analysing the growth of cracks, in particular delaminations, in the laminated composite materials used in wind turbine blades. The Ph.D. project was launched with the following overall purpose:

Establish a framework of rational methods and tools for progressive delamination modeling and simulation of composite laminates in large scale structures under both quasi-static and fatigue loading.

In the following sections of this chapter a description of the background for the project and the motivation for doing this work are given. Then a short introduction to delaminations and how they are modelled is given. Following this, an overall description is given of the level of maturity of the models and methods as well as an presentation of the yet unsolved challenges preventing application of the simulation tools for wind turbine blades.

1.1 Contextual background

The wind energy business has evolved immensely over the last 15 years supported by the high political focus on non-polluting, renewable and independent energy production. Therefore, the current technology of wind turbines has reached a high level of reliability and maturity. Currently, the largest challenge is to reduce the cost of energy production since the cost in general fall behind conventional fossil based energy sources [1]. Thus, a great and ongoing effort is put into reducing the cost of energy from wind turbines. Some focus areas are inspired by the manufacturing practice of the automotive industry where

there is a high degree of automation, modularisation and standardised components while other focus areas fall into classic mechanical engineering tasks of optimizing the wind turbine structure in terms of minimizing the material consumption and cost while ensuring high reliability and robustness. High reliability is of great importance for offshore installations where the cost of repairs is significantly larger than onshore installations. The history shows that the cost of energy decreases with increasing capacity of the wind turbine which is why we see that wind turbines are getting larger.

Siemens Wind Power produces horizontal-axis wind turbines as the one shown in Fig. 1.1. It consists of three blades mounted on a hub which constitute the rotor. The rotor is connected to a generator located in the nacelle. The nacelle is mounted on a tower which is bolted to a foundation. The main loads
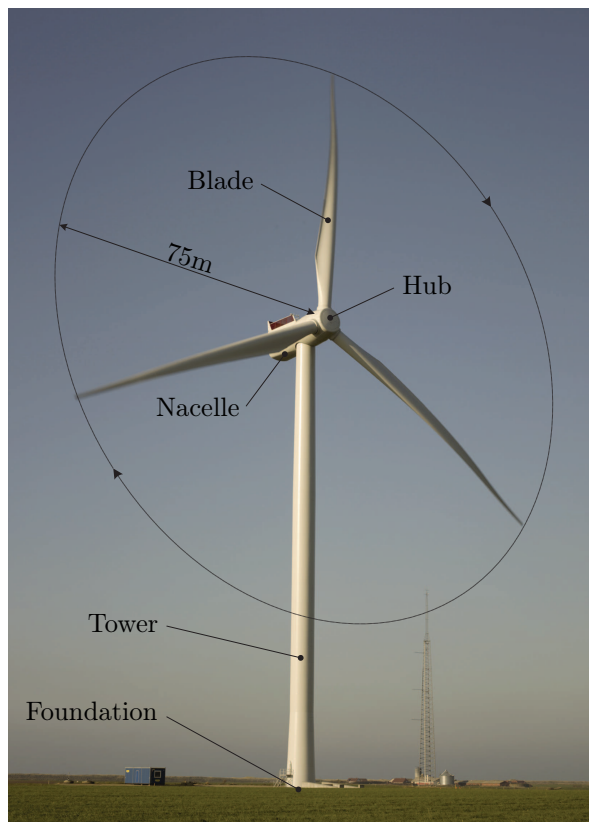
Figure 1.1: SWP wind turbine 6MW direct drive with a rotor diameter of 154m.

on the wind turbine are the wind load and the mass of the structure itself. The blades are important parts to optimize with regards to weight as the mass of the blades will affect the magnitude of loads on all other structural parts of the wind turbine. Thus, lowering the weight of the blades will not just reduce the

material consumption and cost of the blades, but is also a key area for reducing the cost of the remaining structural parts of the wind turbine.

In order to keep a low weight of the blades they are made of composite materials. In Fig. 1.2 a sketch of a generic Siemens Wind Power blade cross section is shown. The structure is hollow and the main load carrying feature
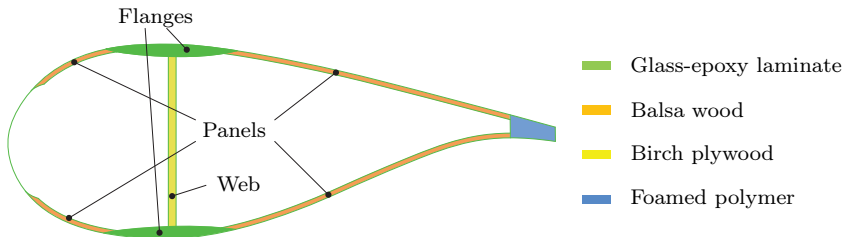
Figure 1.2: Generic cross sectional drawing of a SWP wind turbine blade.

of the blade is the I-beam-like center consisting of flanges made of a glass-epoxy laminated material and a web made of a glass-epoxy-birch ply wood sandwich structure. The panels consist of glass-epoxy-balsa sandwich materials or glass-epoxy laminated composite materials. Sandwich structures are used to increase the bending stiffness of the panels in order to avoid out-of-plane buckling/instability. A more detailed description of these composite materials and structures is given in the following section.

As mentioned previously one of the means to reduce the cost of energy is to reduce the material cost. When this approach to cost reduction is taken it implies utilizing the material to its full capacity. One aspect of this is to take the design closer to the limit of the material which is why it evidently is important to have an accurate knowledge of material limits. This calls for more advanced analysis tools which is the goal of this project.

1.2 Laminated fibrous composite materials and delaminations

The term composite materials describes the combination of two or more materials into a single material to create a material with useful properties. In the case of a Siemens Wind Power wind turbine blades the primary material is glass-epoxy which consists of layers of long continuous glass fiber mats molded into an epoxy resin which holds the fibers in place, see Fig. 1.3.

3

(a)   (b)
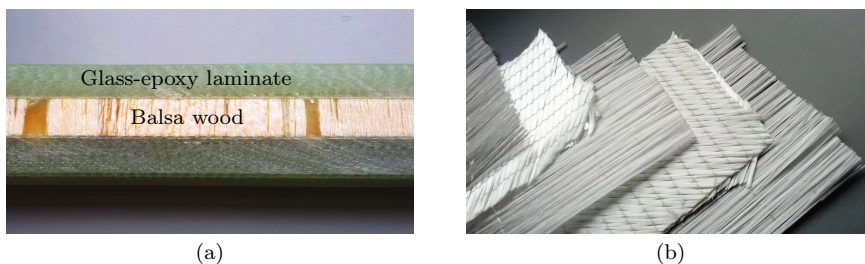
Figure 1.3: (a) Glass-epoxy-balsa sandwich cross section (b) Dry glass fiber mats.

In the direction of the fibers glass-epoxy has a higher stiffness and strength per weight properties compared to conventional structural materials such as steel and aluminium. In contrast to the nice properties in the fiber direction of glass-epoxy the stiffness and strength properties orthogonal to the fiber direction are significantly lower and can be considered the Achilles' heel of laminated composites. In Tab. 1.1 a few selected properties of two typical types of glass-epoxy layers used at SWP are shown which demonstrates this. The reason for the poor properties transverse to the fiber direction is that

	$F_1(t/c)$ [MPa]	$F_2(t/c)$ [MPa]	E_1 [GPa]	E_2 [GPa]
UD	914/525	42/121	43	14
BIAX	150/150	150/150	13	12

Table 1.1: Typical strength and stiffness in the fiber direction (1) and transverse direction (2) of unidirectional (UD) and biaxial (BIAX) glass-epoxy laminates, respectively [2]. The letters t and c denote here tension and compression, respectively.

it basically is the epoxy resin only which carries the load in these directions instead of the strong fibers. In Fig. 1.4 a laminate with 6 UD layers is shown where the strong (1) and weak (2 and 3) directions are indicated.

4
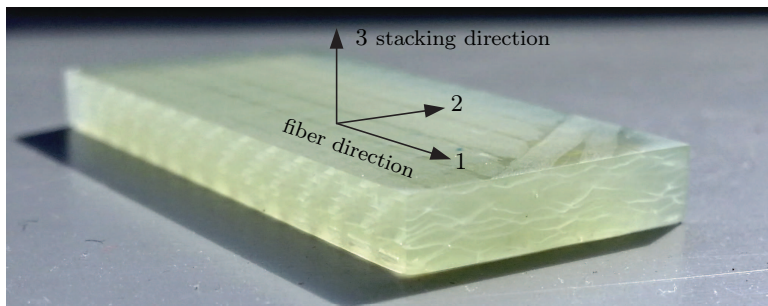
Figure 1.4: Close up on a polished UD laminate where all fibers are oriented in the 1-direction. The white lines in the laminate are sewing tread meant to hold together the fibers until infusion of the epoxy resin is completed.

The nature of composite materials is that it often contains small defects and stress concentrations which can develop into a crack when the material is loaded. Most often these cracks develop in the interface between layers which is the plane given by the 1 and 2 directions in Fig. 1.4. This type of crack is called delaminations and is the type of cracks the methods in the papers of this Ph.D. project focus on. In Fig. 1.5 an example of a delamination in a so-called double cantilevered beam (DCB) specimen is shown. The laminate is similar to the one depicted in Fig. 1.4.
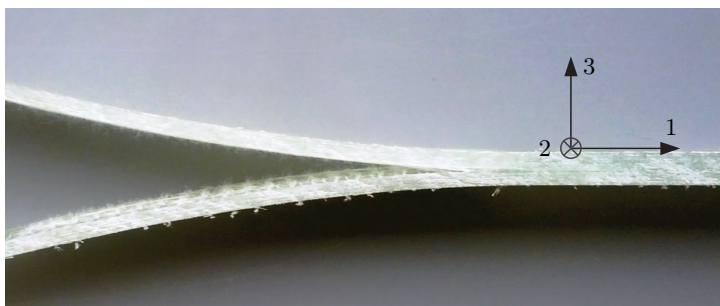
Figure 1.5: A delamination between UD glass-epoxy layers in a DCB specimen.

1.3 Theoretical background

There are two main fracture mechanical frameworks which are suited for the type of delamination simulation studies in focus. These frameworks are linear elastic fracture mechanics (LEFM) and cohesive zone modelling (CZM). The choice of using cohesive zone models as the point of departure was made from the very beginning of this project. However, both frameworks possess advantages and challenges. One of the advantages of cohesive zone models, which is

one of the main reasons for using this framework, is that they enable a highly automated analysis of delamination propagation without the need for geometry and mesh changes when they are used in connection with finite element analysis.

In the following sections an introduction to the topic of cohesive zone models used for delamination analysis is given. The introduction serves as an overview and leads to the formulation of unsolved challenges of applying these current available methods for delamination analysis in large structures.

1.3.1   Basic properties of cracks and growth of cracks

In a continuum mechanics setting a crack is modelled as a surface of discontinuity S of the continuum, see Fig. 1.6. In the unloaded state of the continuum the opposing surfaces S^- and S^+ are coincident and denoted the crack faces. The continuum on each side of the crack cannot penetrate which means that only compressive normal tractions and friction shear tractions can be transferred between the crack faces. All other tractions on the crack faces are zero.
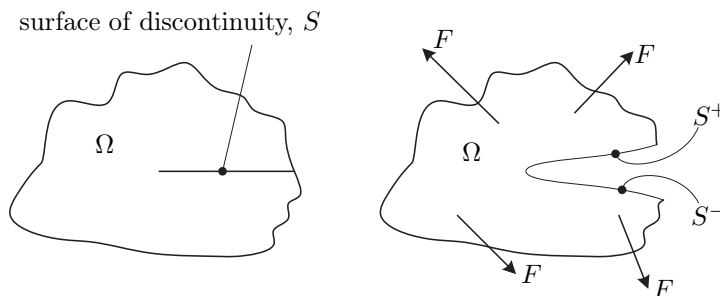
Figure 1.6: Crack modelled as a surface of discontinuity S in a continuum defined as the domain Ω.

One of the fundamental understandings of the growth of cracks was formulated by Griffith [3] who formulated a crack growth criterion for elastic bodies which assumes that crack growth is an energy dissipating process where the energy needed to increase the crack area A is assumed to be a constant material property. This material property has later been refereed to as the critical energy release rate $\mathcal{G}_c$.

For delamination cracks in layered composites the critical energy release rate $\mathcal{G}_c$ cannot be considered solely a material constant since it is dependent on for example the crack loading configuration. Even so the basic idea of considering the energy dissipation per crack area a constant material property is maintained with some additions/corrections which are described in Sec. 1.3.5.

1.3.2 Cohesive zone modelling and cohesive laws

The first practical framework for general analysis and modelling of cracks was linear elastic fracture mechanics (LEFM) [4] which is based on linear elasticity. The LEFM framework leads to infinite strains and stresses at the crack tip which are artifacts of using linear elasticity and assuming an infinitely sharp crack tip. As infinite stresses at the crack tip do not hold a physical meaning and as the linear elastic assumptions of small deformations and rotations are violated in the solution, Barenblatt [5] worked on an alternative formulation which ensures finite stresses at the crack tip. The work took point of departure in linear elasticity and Barenblatt argumented that the only way to avoid infinite stresses is to have a traction field in front of the crack tip which exactly balances out the crack opening force, see Fig. 1.7. The extend of the cohesive tractions is defined as the cohesive zone length.
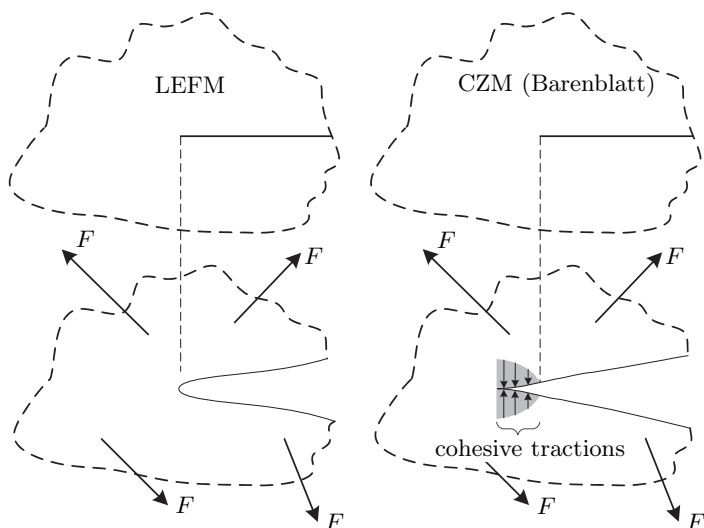
Figure 1.7: a LEFM crack and a CZM (Barenblatt) crack in (upper) unloaded and (lower) loaded configuration, respectively.

A consequence of avoiding the infinite stresses by this traction field is that it results in a smooth cusp like joining of the crack faces[1]. This implies that the local rotational deformation at the crack tip is zero unlike in the LEFM where the crack faces are rotated $\pi/2$ at the crack tip.

Barenblatt claimed that the cohesive tractions holding together the crack faces in front of the crack tip are due to atomic forces in the material which are a function of the separation length of the atoms. Since then the physical interpretation of what leads to these cohesive tractions have been adapted to different

---

[1]Note that Barenblatt [5] only considered normal separation of the crack faces.

material systems, where some of the most relevant for delamination damage of fibrous composites are: fiber bridging [6–9], polymer crazing/bridging [10], small scale yielding [11] and micro cracks close to the crack tip [12, 13], see Fig. 1.8.
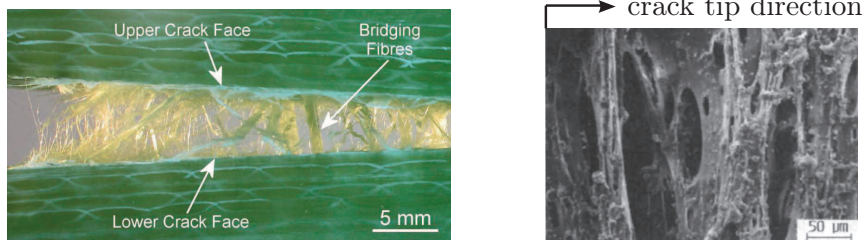
Figure 1.8: Mechanisms leading to cohesive tractions. Left: fiber bridging [9]. Right: Polymer Tearing.

Common for all available cohesive laws is that they are constitutive laws relating the crack face separation displacement vector, $\boldsymbol{\delta}$ to the traction vector $\boldsymbol{\tau}$ and that they have a negative slope as shown in Fig. 1.9.
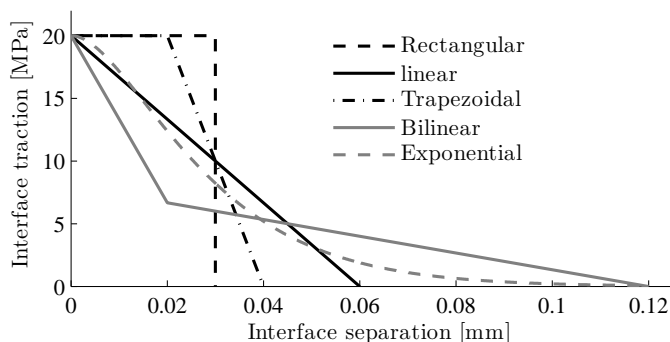
Figure 1.9: Different common representations of a cohesive law. Rectangular [11], Linear [14], Trapezoidal [15], Bilinear [16], Exponential [17]. All the depicted cohesive laws are shown with the same maximum traction τ_o and critical energy release rate $\mathcal{G}_c$

Rice [18] used the J-integral to show that the total specific work of the cohesive tractions (the area below the cohesive law curve) is equal to the critical energy release rate of the material $\mathcal{G}_c$.

It is difficult to measure cohesive laws in general because of the small length-scale associated with the cohesive forces. Only a few methods exist for determination of cohesive laws in composite materials. One of these is the method by Sørensen [19]. The method relies on determination of the J-integral [18] as a

function of the crack face separation and differentiation of experimental data. Thus, in order to get meaningful results a high degree of filtering of the data and curve fitting with simple curves are used. The choice of filtering and curve fitting have significant effect on the shape of the cohesive law which is why it is best suited for determining large scale bridging tractions and not the cohesive tractions in the close vicinity of the crack tip. The method can be used to determine basic properties of the cohesive law with meaningful accuracy like the overall shape and the critical opening δ_c which is defined as the opening above which, the crack faces are free of tractions. However, the maximum traction and the shape close to zero opening are not possible to determine with current experimental methods. Instead the bulk material strength of the interface is used which is further explained in section 1.3.3.

As a part of a Ph.D. course in fracture mechanics for laminated composite structures [20] at Aalborg University, which the author co-organized, the cohesive law for an interface between UD glass-epoxy was determined using the approach of [19]. This is shown here to demonstrate the difficulties in determining the whole cohesive law.

Based on the applied moment the J-integral can be determined and the interface separation is measured using a clip-gauge, see Fig. 1.10.
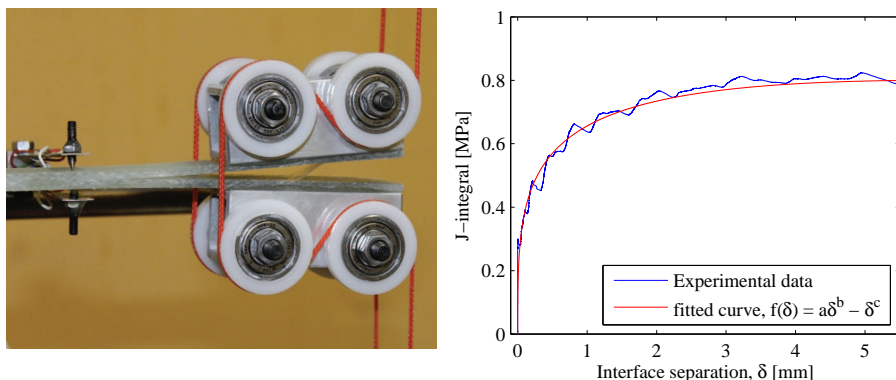
Figure 1.10: Test setup and data for determination of the cohesive law of an interface between UD glass-epoxy.

The cohesive law is then obtained by differentiating the smooth fitted curve of the experimentally obtained J-integral data with respect to the interface opening, see Fig. 1.11. It is seen that the crack faces are free of tractions once the opening increases above the critical opening δ_c at 6 mm and also that the tractions are reduced to 0.5 MPa at the interface separation $\delta = 0.24$ mm.
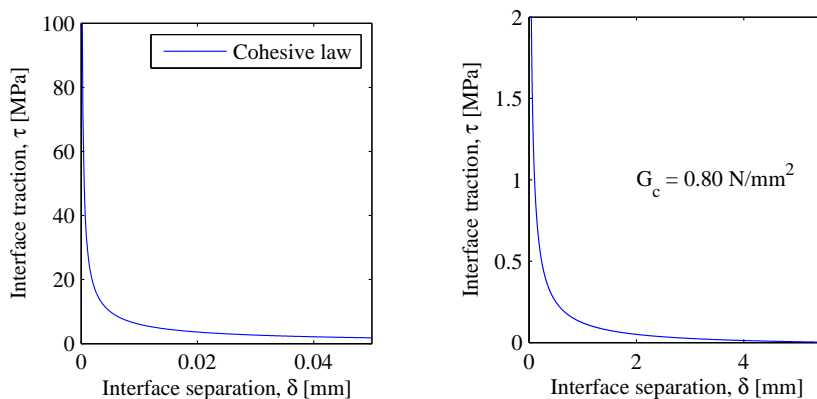
Figure 1.11: The cohesive law determined by differentiation of the fitted J-integral curve with respect to the interface opening.

An important property to note about the shape of the cohesive law is the large change in traction for openings in the interface separation interval $\delta \in]0, 0.1]$ mm. The length scale of this opening is very small compared to the structural scale of wind turbine blades or even the thickness of the laminate. This large difference in length scale is in fact one of the main challenges when applying CZMs to large structures since it makes solving the problem computationally heavy. This length scale challenge will be discussed further in section 1.4.

1.3.3   Potential crack paths and initiation of new cracks

Since cracks in the interface between fiber layers in many situations are confined to propagate in the interface only, the potential crack path approach of Needleman [21, 22] can be used. Using this approach each fiber layer is modelled as a separate body and each body is then held together to the adjacent bodies by cohesive tractions, see Fig. 1.12.
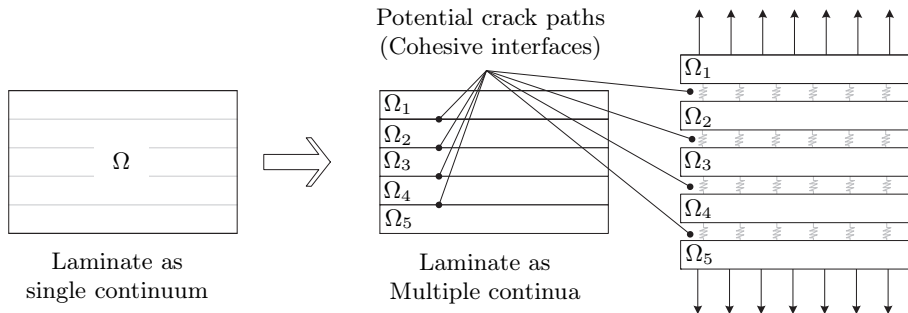
Figure 1.12: Needleman's potential crack path approach. The laminate defined by domain Ω is split along all potential crack paths into subdomains Ω_1 to Ω_5 and held together by cohesive tractions.

When cohesive laws are used in predefined crack paths as depicted in Fig. 1.12 the laws are formulated with an initial elastic hardening, see Fig. 1.13. In this way the cohesive law has a positive stiffness up to the maximum traction after which the stiffness is negative[2].
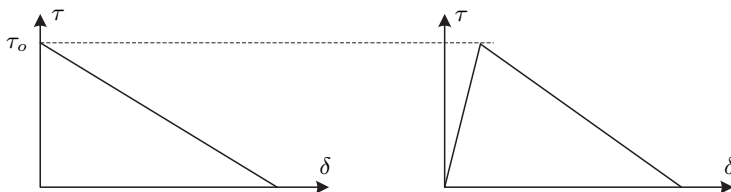
Figure 1.13: Cohesive laws with initial hardening used with the potential crack path approach [21, 22].

The initial positive stiffness is introduced even though the thickness of the interfaces are zero which would call for a rigid cohesive law until the onset traction is reached [24]. Allowing the initial positive stiffness enables that the tractions on the crack faces can be evaluated based on the crack face separation only which is practical when applied in finite element analysis. The system behaves more compliant doing this, but the influence can be reduced to an insignificant size by ensuring a high initial stiffness in relation to the material stiffness of the surrounding laminate [25].

Hillerborg [12] suggested that the maximum traction, also denoted the onset traction τ_o, can be considered equal to the material strength in the absence of a crack. When this approach is taken cohesive zone models can also be used to predict the initiation of cracks in pristine laminates. In many cases strength

---

[2]Cohesive laws which are rigid until the onset traction is reached is also refereed to as extrinsic cohesive models and cohesive laws with an initial positive stiffness are refereed to as intrinsic cohesive models [23].

of materials and fracture mechanical properties cannot be related, however numerous studies e.g. [18, 26, 27] have shown that the critical energy release rate is the single governing parameter when the extend of the crack is large compared to the length of the cohesive zone. Furthermore, as mentioned previously, the current experimental characterization techniques of cohesive zone laws are not yet capable of determining the cohesive law for very small interface separations which is needed in order to determine the onset traction. Thus, it seems that the cohesive zone models following the approach of Needleman [21] and Hillerborg [12] are cable of simulating both initiation and propagation of cracks without compromising either one capability.

The combination of the approaches of Needleman [21] and Hillerborg [12] enables a very automated simulation of initiation and propagation of delaminations and is relatively easy to implement in a finite element framework.

1.3.4 Damage and irreversible crack propagation

In order to ensure irreversible crack propagation in the cohesive zone model formulation, the damage parameter concept known from continuum damage mechanics is applied. In the following an overall figurative introduction to damage in cohesive zone models is given. The details of the specific formulation used in paper A and C are presented in section 1.3.6.

In Fig. 1.14 a sequence of loading and unloading of a crack modelled with a cohesive zone model is shown. The opening and traction of the location in the crack interface marked with a dot is traced on the cohesive law. Initially (a) there is no damage at the location of the dot. When the crack is loaded above the onset of propagation (b) the traction-separation relation follows the softening part of the cohesive law and the damage is updated accordingly. If the crack is then unloaded (c) the traction-separation relation follows a linear curve to the origin. As long as the traction-separation relation follows this curve the damage variable remains constant. If the crack is loaded again the traction-separation relation will follow the updated cohesive law shown in (d).

During the loading-unloading in (b)-(c) energy is dissipated which is indicated in grey and the remaining ability to do non-conservative work is marked with blue, see Fig. 1.15. The curve around the blue area also represents the updated cohesive law after damage.
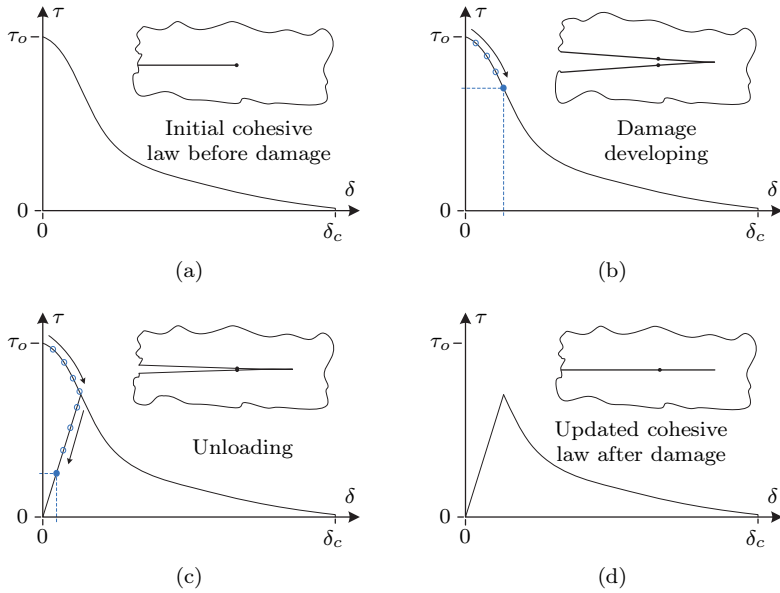
Figure 1.14: Sequence showing damage development during crack growth.
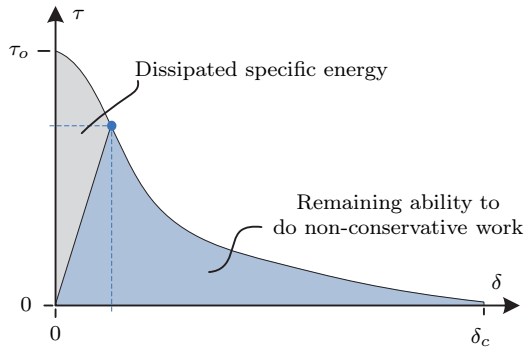
Figure 1.15: Updated cohesive law after damage

1.3.5 Crack loading modes and bimaterial cohesive interfaces

In the case of glass-epoxy and most other materials the critical energy release rate is not purely a material constant, but is also a function of the way the crack is loaded. A crack can be loaded in a combination of the three basic opening modes shown in Fig. 1.16. Mode I is a symmetric normal opening

about the crack plane, Mode II is an in-plane shear opening and mode III is an out-of-plane shear opening.

| Unloaded | Mode I | Mode II | Mode III |
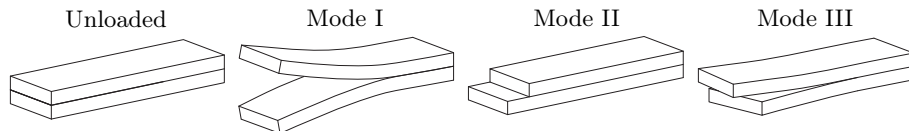
Figure 1.16: The three basic crack opening modes.

In most conventional structural materials like metals a crack loaded in a combination of mode II or mode III will change direction during propagation until mode I loading is reached. This is because mode I in general is the least energy dissipating opening mode and because this energy dissipation is independent of the orientation of the crack in relation to the material. However, in laminated composites the crack is often bounded to propagate in the interface; even under mixed mode conditions dominated by mode II and III. As an example, the values of the critical energy release rate for a SWP UD glass-epoxy laminate with the crack propagating along the fiber direction are $\mathcal{G}_{Ic} = 613$ J/m^2 in mode I and $\mathcal{G}_{IIc} = 2252$ J/m^2 in mode II.

As mentioned previously delaminations propagate under mixed mode in general since they are confined to propagate in the interface between fiber layers. There are two reasons for why crack propagation under mixed mode occurs. One reason is mixed outer loading as shown in Fig. 1.16. Another reason is the different elastic properties of adjacent layers [28], e.g. due to different fiber orientations or weaves. In fact the different elastic properties of adjacent layers can lead to mixed mode crack opening locally at the crack tip even though an outer mode I opening is applied. Cracks between two different materials are denoted bimaterial interface cracks and have been given much attention and is well described in the framework of LEFM, but not in the framework of cohesive zone models. The reason that careful treatment of mode mixity is important is that both crack propagation under quasi-static and fatigue loading is influenced by the mode mixity. The critical energy release rate $\mathcal{G}_c$ [29], the interface strength τ_o [2], and crack growth rate in fatigue [30] are all functions of the mode mixity during propagation and can only be determined experimentally.

When considering cohesive zone models, which are capable of handling a general (experimentally determined) mode mixity dependency, there are two relevant definitions of the mode mixity. These mode mixity definitions are:

- Mode mixity ϕ expressed by the mode decomposed energy release rates $\mathcal{G}_I$, $\mathcal{G}_{II}$ and $\mathcal{G}_{III}$ [31, 32]

- Mode mixity β expressed by normal and tangential crack faces separations $\delta_I, \delta_{II}, \delta_{III}$ [33, 34]

The interface separation based mode mixity β is not unique for a given load scenario like the energy release rate based mode mixity ϕ, but varies through the cohesive zone [35–37]. Numerical studies show that the variation of β through the cohesive zone is problem dependent since it is influenced by the geometry of the structure and material stiffnesses. Thus, there is no relation between the energy release rate based mode mixity ϕ definition and the pointwise displacement based mode mixity β. This can lead to some confusion since the experimental data of the critical energy release rate $\mathcal{G}_c$ used for mixed mode cohesive laws are extracted using the energy release rate based mode mixity definition ϕ and applied in a CZM using the crack face separation based mode mixity definition β.

There exist different approaches to formulate mode mixity capable cohesive laws such as models with decoupled mode I and II, potential based models, and the models treated in this project which are equivalent one dimensional laws. The latter type of CZMs relates the norm of the displacement jump to the norm of the traction [38]. No matter which type of formulation of the mixed mode law is used, the energy dissipation will be path dependent unless certain relations of $\mathcal{G}_{Ic}$, $\mathcal{G}_{IIc}$, τ_I^o, and τ_{II}^o are maintained [24, 35, 39, 40]. In fact, the only way to make sure that there is no path dependency of the energy dissipation in the general case is to have $\mathcal{G}_{Ic} = \mathcal{G}_{IIc} = \mathcal{G}_{IIIc}$ and $\tau_I^o = \tau_{II}^o = \tau_{III}^o$. This means that in fibrous laminated composite interfaces where there are significant differences of the critical energy release rates and the interface strengths, mode mixity simulation results will in general be path dependent.

All cohesive models are isotropic, in the sense that strengths τ_{Io}, τ_{IIo} and τ_{IIIo} and the critical energy release rates $\mathcal{G}_{Ic}$, $\mathcal{G}_{IIc}$ and $\mathcal{G}_{IIIc}$ are independent of the crack propagation direction and the orientation of the materials adjacent to the cohesive interface. As the current cohesive models are not dependent on crack propagation orientation the two shearing modes II and III cannot be separated and is instead treated as a single shear mode.

1.3.6 Resume of the applied cohesive zone model

The cohesive zone model for quasi-static modelling which forms the basis of the work done in paper A and C are the model of Turon [34] which is an extension of the model of Camanho [33]. The basic features of the formulation are described in the following.

The model is based on the potential crack path approach by [21] as described in section 1.3.3. At the interface, the coincident surfaces of each body part separated are denoted S^+ for the surface associated with the upper body and similarly S^- for the lower body. In the deformed configuration, the separation of the two parts of the deformed body is described in a local Cartesian coordinate system, $(\boldsymbol{e}^1, \boldsymbol{e}^2, \boldsymbol{e}^3)$ located on the middle surface, $\bar{S}$, see Fig. 1.17.

The middle surface in the deformed configuration is defined as the average distance between initially coinciding points at the upper and lower surface of
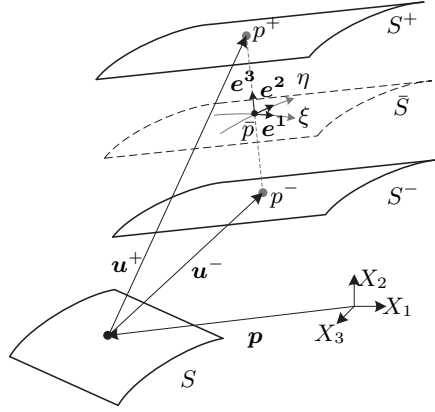
Figure 1.17: Description of the middle surface $\bar{S}$ in the deformed configuration.

the undeformed body and is in the global Cartesian coordinates (X) defined as:

$$\bar{\boldsymbol{x}} = \boldsymbol{p} + \frac{1}{2}(\boldsymbol{u}^+ + \boldsymbol{u}^-) \tag{1.1}$$

The separation of two initially coinciding points at the interface in the global Cartesian coordinate system is defined as:

$$\boldsymbol{u}^+ - \boldsymbol{u}^- \tag{1.2}$$

The local coordinate system $(\boldsymbol{e}^1, \boldsymbol{e}^2, \boldsymbol{e}^3)$ is derived from a curvilinear coordinate system (η, ξ) located on the middle plane in the following way:

$$\boldsymbol{v}^\xi = \frac{\partial \bar{\boldsymbol{x}}}{\partial \xi} \qquad \boldsymbol{v}^\eta = \frac{\partial \bar{\boldsymbol{x}}}{\partial \eta} \tag{1.3}$$

$$\boldsymbol{e}^1 = \frac{v^{\boldsymbol{\xi}}}{|v^{\boldsymbol{\xi}}|} \qquad \boldsymbol{e}^3 = \frac{\boldsymbol{v}^\xi \times \boldsymbol{v}^\eta}{|\boldsymbol{v}^\xi \times \boldsymbol{v}^\eta|} \qquad \boldsymbol{e}^2 = \boldsymbol{e}^3 \times \boldsymbol{e}^1 \tag{1.4}$$

The curvilinear coordinate axes, η and ξ, are in general not orthogonal which is why only $\boldsymbol{e}^1$ and $\boldsymbol{v}^\xi$ are parallel. The transformation tensor between global and local coordinates, $\boldsymbol{\Theta}$, is:

$$\boldsymbol{\Theta} = \begin{bmatrix} e_1^1 & e_2^1 & e_3^1 \\ e_1^2 & e_2^2 & e_3^2 \\ e_1^3 & e_2^3 & e_3^3 \end{bmatrix} \tag{1.5}$$

Thus, the separation in local coordinates $(\boldsymbol{e}^1, \boldsymbol{e}^2, \boldsymbol{e}^3)$ is given as:

$$\boldsymbol{\delta} = \boldsymbol{\Theta}(\boldsymbol{u}^+ - \boldsymbol{u}^-) \tag{1.6}$$

where $\boldsymbol{\Theta}$ is the transformation tensor between the global and local coordinate system. The constitutive relation between the displacements $\boldsymbol{\delta}$ and tractions $\boldsymbol{\tau}$ between the crack faces S^+ and S^- are defined as:

$$\tau_i = (1 - D^k)K\delta_i \qquad \text{for} \quad i = 1, 2$$
$$\tau_3 = (1 - D^k)K\delta_3 - D^k K \frac{1}{2}(-\delta_3 + | -\delta_3|) \tag{1.7}$$

where the scalar damage variable D^k is a measure of the state of damage of the interface. D^k is defined in the interval $[0, 1]$ and describes the linear reduction of the initial constitutive unloading stiffness K. The evolution of D^k is controlled by a cohesive law and a damage model which are expressed by an equivalent one dimensional opening displacement λ and an equivalent one dimensional interface traction μ:

$$\lambda = \sqrt{(\delta_I)^2 + (\delta_s)^2} \qquad \delta_I = \frac{1}{2}(\delta_3 + |\delta_3|) \qquad \delta_s = \sqrt{(\delta_1)^2 + (\delta_2)^2}$$
$$\mu = (1 - D^k)K\lambda \tag{1.8}$$

where δ_I is related to mode I crack opening and δ_s is a shear opening related to a combined mode II and III crack opening (mode II and III are not distinguished). It is assumed that the negative normal opening (penetration of crack faces) does not affect damage development. Thus, δ_I is set equal to zero when the crack faces penetrate. Based on the equivalent one dimensional opening displacement λ and interface traction μ, an equivalent single mode cohesive law can be defined. This is shown in Fig. 1.18 and is used to determine the damage which is needed to determine the interface traction $\boldsymbol{\tau}$ in Eq. (1.7). μ_o is the equivalent one dimensional onset traction, (δ_D, μ_D) is the equivalent one dimensional opening and traction associated with the current damage D^k and mode mixity β, $\mathcal{G}_c$ is the critical energy release rate, and w_{tot} is the total specific work.
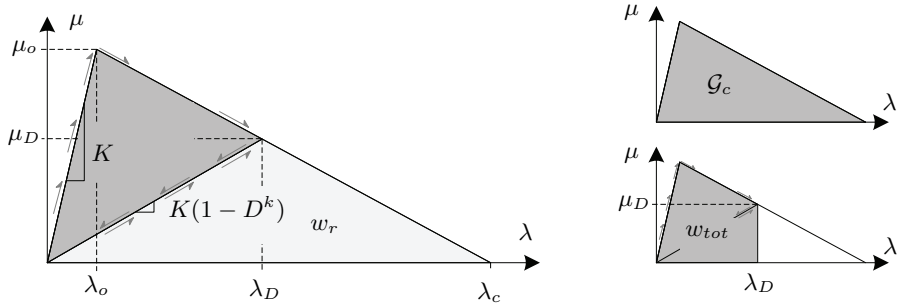

Figure 1.18: Equivalent single mode cohesive law for mixed mode three dimensional quasi-static delamination propagation simulation. The cohesive law is shown for a constant mode mixity.

λ_o and λ_c are the equivalent one dimensional onset and critical openings, respectively, and are given by:

$$\lambda_o = \frac{\mu_o}{K}, \qquad \lambda_c = \frac{2\mathcal{G}_c}{\mu_o} \tag{1.9}$$

w_r is the specific remaining ability to do non-conservative work and is defined as:

$$w_r = \frac{1}{2}\lambda_D(1 - D^k)K\lambda_c \tag{1.10}$$

The critical energy release rate $\mathcal{G}_c$ and the equivalent single mode onset traction μ_o are determined using a modified BK-criterion [29, 34] expressed in the local opening displacement based mode mixity β. This is different from the mode mixity ϕ used in Paris' Law which is defined by the mode decomposed energy release rates $(\mathcal{G}_I, \mathcal{G}_{II}, \mathcal{G}_{III})$.

$$\begin{aligned} \mathcal{G}_c &= \mathcal{G}_{Ic} + (\mathcal{G}_{IIc} - \mathcal{G}_{Ic})B^\eta \\ \mu_o &= \sqrt{(\tau_{Io})^2 + [(\tau_{IIo})^2 - (\tau_{Io})^2]B^\eta} \\ \text{where} \quad B &= \frac{\beta^2}{2\beta^2 - 2\beta + 1} \quad \text{and} \quad \beta = \frac{\delta_s}{\delta_I + \delta_s} \end{aligned} \tag{1.11}$$

where subscripts I and II denote the pure mode I and II values, respectively, and η is a mode interaction parameter. The damage criterion presented in [34] has been extended with the explicit dependency of the mode mixity β as, in general, it is changing continuously through the cohesive zone. The extension is done using the formulation in [41]. The criterion for the evolution of the damage variable D^k is defined as:

$$s - r \leq 0 \tag{1.12}$$

where r is the threshold for damage evolution. The criterion implies that the damage state is unchanged if $s - r < 0$. If $s - r = 0$ damage can, but does not necessarily, evolve. The variables r and s are defined as:

$$\begin{aligned} s &= \frac{\lambda_c[\lambda - \lambda_o]}{\lambda[\lambda_c - \lambda_o]} \\ r = \frac{\lambda_c[\lambda_D - \lambda_o]}{\lambda_D[\lambda_c - \lambda_o]} \quad &\text{where} \quad \lambda_D = \frac{\lambda_o\lambda_c}{\lambda_c - D^k[\lambda_c - \lambda_o]} \end{aligned} \tag{1.13}$$

where λ_D is the equivalent one dimensional opening corresponding to the current damage state at a given mode mixity β. The function r is formulated such that the evolution of the damage variable D^k is defined as $\dot{D}^k = \dot{r}$. It is assumed that the evolution of the damage variable is irreversible, meaning that $\dot{d} \geq 0$ and thereby $\dot{r} \geq 0$. The latter implies that the threshold for damage evolution r and thereby the damage variable D^k can be determined as the so far maximum value of s less than or equal to one:

$$D^k = r = \min(\max(0, s), 1) \tag{1.14}$$

If a crack is propagating, the criterion for evolution of the damage state in Eq. (1.12) is met, meaning that $r = s$. It then follows that $\lambda_D = \lambda$ which is used later in the fatigue damage rate model presented in paper C.

1.3.7 Finite element formulation

In order to conduct analyses of delamination propagation numerical methods are needed. All recent cohesive zone models for delamination propagation simulations have been implemented in a finite element framework. These implementations are typically based on contact formulations, solid elements or zero thickness interface elements. The present work is based on zero thickness interface elements since interfaces between fiber layers in the materials considered here have insignificant thickness and since the contact based formulations are less robust and therefore acquire a higher computational effort.

The works in papers A and C are based on an 8-noded element with interpolation functions defined on the middle surface $\bar{S}_e$ extended by the η and ξ curvilinear coordinate vectors, see Fig. 1.19.
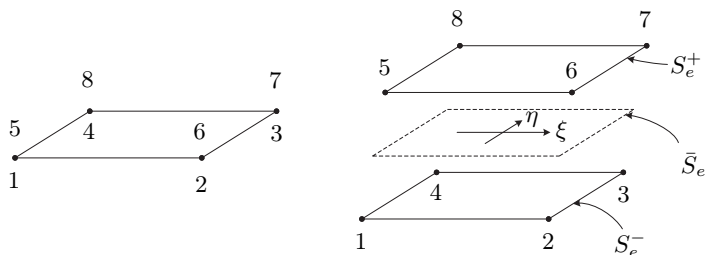
Figure 1.19: Zero thickness brick element in (left) undeformed configuration and (right) exploded view. The numbering of nodes is shown.

The opening displacements $\boldsymbol{\Delta}$ in the element are defined as:

$$\boldsymbol{\Delta} = \boldsymbol{\Theta N q} \tag{1.15}$$

where $\boldsymbol{N}$ is the interpolation function matrix and is assembled such that the displacements of the upper crack face S_e^+ are subtracted from the displacements of the lower crack face S_e^-. The vector $\boldsymbol{q}$ contains the nodal displacements. The shape function matrix $\boldsymbol{N}$ is given as:

$$
\begin{aligned}
N_1 &= \frac{1}{4}(1-\xi)(1-\eta), & N_2 &= \frac{1}{4}(1+\xi)(1-\eta) \\
N_3 &= \frac{1}{4}(1+\xi)(1+\eta), & N_4 &= \frac{1}{4}(1-\xi)(1+\eta)
\end{aligned}
\tag{1.16}
$$

$$\boldsymbol{N}^+ = \begin{bmatrix} N_1 & 0 & 0 & & N_4 & 0 & 0 \\ 0 & N_1 & 0 & \cdots & 0 & N_4 & 0 \\ 0 & 0 & N_1 & & 0 & 0 & N_4 \end{bmatrix}$$
$$\boldsymbol{N}^- = -\boldsymbol{N}^+ \qquad\qquad\qquad\qquad\qquad (1.17)$$
$$\boldsymbol{N} = [\boldsymbol{N}^-, \boldsymbol{N}^+]$$

The element internal force vector expressed in global coordinates can be derived from the principle of virtual work and Newton's third law [42]:

$$\boldsymbol{f} = \int_{\bar{S}_e} \boldsymbol{N}^T \boldsymbol{\Theta}^T \boldsymbol{\tau} d\bar{S}_e = \int_\xi \int_\eta \boldsymbol{N}^T \boldsymbol{\Theta}^T \boldsymbol{\tau} |\boldsymbol{v}^\xi \times \boldsymbol{v}^{\boldsymbol{\eta}}| d\eta d\xi \qquad (1.18)$$

where $\bar{S}_e$ is the middle surface of the element in the deformed configuration. The complete element tangent stiffness matrix is determined as the first derivative of the residual which in this case is the element internal force vector with respect to the nodal displacements. In order to reduce the complexity of the implementation the terms related to changes of the mode mixity, changes of the transformation matrix and changes in the deformed interface area with respect to displacements are all omitted such that the element stiffness matrix $\boldsymbol{K_t}$ is calculated as:

$$\boldsymbol{K_t} \approx \int_{\bar{S}_e} \boldsymbol{N}^T \boldsymbol{\Theta}^T \boldsymbol{D}^{\tan} \boldsymbol{\Theta} \boldsymbol{N} d\bar{S}_e = \int_\xi \int_\eta \boldsymbol{N}^T \boldsymbol{\Theta}^T \boldsymbol{D}^{\tan} \boldsymbol{\Theta} \boldsymbol{N} |\boldsymbol{v}^\xi \times \boldsymbol{v}^{\boldsymbol{\eta}}| d\eta d\xi \quad (1.19)$$

The integrals of $\boldsymbol{f}$ and $\boldsymbol{K_t}$ are evaluated using numerical integration methods such as Newton-Cotes quadrature and Gauss-Legendre quadrature which is treated in detail in paper A.

1.3.8 Fatigue models

The loads on a wind turbine blades can overall be divided into wind loads and inertia loads from rotation of the rotor. The typical service life of modern wind turbines is 20 years. This leads to a total number of revolutions of approximately $2 \cdot 10^8$ which is why the focus on fatigue is limited to high-cycle fatigue. The load time history of a wind turbine is highly varying and appears almost random with no easy identification of mean or amplitude of the load variation. Furthermore, it is difficult to mimic a realistic load spectrum in controlled design verification tests of full wind turbine blades. Thus, in order to make fatigue simulations and tests operational the real load spectrum is converted to an equivalent constant cycling load that for a certain number of cycles is assumed to produce the same damage or crack growth [43]. The approach is based on Palmgren-Miner linear damage hypothesis [44, 45] and a cycle count approach such as rainflow counting [46].

The models used for experimental characterization of high-cycle fatigue delamination growth in composite materials are all variants of Paris' law [47].

By variants of Paris' law is meant that the crack growth rate da/dN, where a is the crack length and N is the number of load cycles, is a function expressed in LEFM quantities. These LEFM quantities are the mode mixity and the amplitude and mean value of either the stress intensity K or the energy release rate $\mathcal{G}$. As mentioned previously only the energy release rate approach is relevant for cohesive zone models.

The mean and amplitude of the energy release rate are functions of the loading of the crack at the minimum and maximum of the cyclic varying load, see Fig. 1.20 where this is exemplified by a moment loaded DCB specimen. The minimum and maximum loads are also denoted the load envelope.
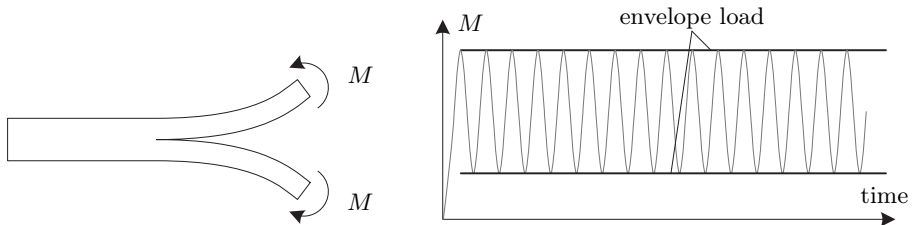
Figure 1.20: The envelope load approach exemplified by a moment loaded DCB specimen.

Similar to these experimental characterization models there is a class of cohesive zone models for high-cycle fatigue which is denoted envelope load models [48–50]. The novel fatigue model and method presented in Paper C is based on the envelope load model approach. The cohesive models based on the envelope load models for fatigue crack growth simulation are formulated as damage rates dD/dN instead of crack growth rates da/dN. Since there does not exist any experimental characterization of the damage, all available models in the literature are either approximately linked to or calibrated using a variant of Paris' law.

Assuming that a structure behaves geometrically and material-wise linear the cyclic variation of the energy release rate, and thereby the crack growth rate, can be determined from the maximum energy release rate and the load ratio R of the outer load applied to the structure. Since the maximum energy release rate is occurring at the maximum outer load the fatigue crack growth analysis can be conducted in a quasi-static manner where only the maximum outer load is applied to the structural model.

1.4 The challenges and research objectives addressed

As described in the beginning of this chapter the overall purpose of the Ph.D. project is reliable and computational efficient methods for delamination under quasi-static and fatigue loading. As described in the previous sections the level of maturity of the methods for delamination propagation simulation as a result

of quasi-static loading and fatigue loading, respectively, are at very different levels. The methods for quasi-static delamination simulation are well consolidated in the way that the methods are well-described and have been used in advanced simulations such as simulation of a complete main spar of a wind turbine blade [51]. As described in paper B, the methods for fatigue-driven delaminations are all very recent and the models and methods are not yet mature enough to be relevant for industrial application. Because of this difference of the two fields the contributions fall into different categories. The work on quasi-static methods is focused on computational cost while the work on fatigue methods are focused mainly on extending the capabilities and accuracy and secondly the computational cost when applying the methods for numerical simulation.

In regards to methods for quasi-static loading there are two main areas which needs further development. One is the high computational cost of running analyses and the other is limited capabilities in regards to mixed mode crack propagation. Since all the cohesive zone model based fatigue models and methods are extensions of quasi-static models, these areas that need further development also apply to the methods and models for fatigue loading as well.

As mentioned in the previous section the issues in regards to mixed mode capabilities are an unintended structural and material dependency of the energy dissipation under mixed mode crack opening. Furthermore, there are some issues in relation to three dimensional crack propagation which include the missing ability to distinguish shear opening displacement into mode II and mode III, respectively. Also the current models are not able to take into consideration the critical energy release rate as a function of the orientation of the crack front in regards to material orientation. However, one of the largest challenges preventing the application of delamination simulation methods in the design work for SWP is the high computational effort associated with the methods when the structures being analysed are as big as a wind turbine. This stems from the mesh density requirement of having at least 3 to 10 elements (depending on material and structure) in the damage process zone. The order of magnitude of the damage process zone is practically independent of the size of the structure meaning that it will be in the range of approximately 5mm to 10mm. There is a large difference in length scales between the structural level (currently up to 75 m long) where loads are introduced and the size of the damage process zone. This means that even with the use of multi-scale analysis (also known as sub-modelling) [?] the degrees of freedom in the system becomes very large and with it the computational cost.

In regards to methods for simulating fatigue driven delaminations several areas in the need of further development because of the low level of maturity of this topic. The main areas in need of further development in relation to fatigue driven delamination simulations in large structures are the predictive capabilities and accuracy of the simulations and similar to the quasi-static methods the computational efficiency.

Chapter 2

Description and conclusions of the papers

In this chapter extended summaries of the three main papers of the Ph.D. work are given. Following the summaries the contributions and impact of the work as a whole are described.

2.1 Paper A

Paper A with the title *Analysis of the Integration of Cohesive Elements in regards to Utilization of Coarse Mesh in Laminated Composite Materials* [52] presents an analysis of the influence of the integration error introduced by the numerical integration of the internal force and stiffness matrix of cohesive elements used in finite element analysis of delamination propagation. The influence is measured in terms of ability to converge to a solution, number of equilibrium iterations needed to converge to a solution (computational time), and error in the obtained solution.

A means to obtain a higher computational efficiency is to reduce the number of elements in the finite element model which results in a lower resolution of elements in the cohesive zone at the delamination front. However, in models with a low element resolution in the cohesive zone, a oscillating response can be observed in the obtained solution. An example of this is shown in Fig. 2.1 for a double cantilevered beam, specimen model. Further details of the model is given in the paper.

It is shown in the paper that the two main reasons for the oscillating response are the size variation of the cohesive zone following from discretization of the displacement field and integration error of the element force vector and stiffness matrix. Based on a simulation of the entire opening history of a single 3 mm cohesive element with it is demonstrated that the commonly used 2×2 Newton-Cotes quadrature introduces a large error in the calculation of the element force vector and stiffness matrix. In the study the relative error of the nodal normal force is between -750% and 1654% using 2×2 Newton-Cotes
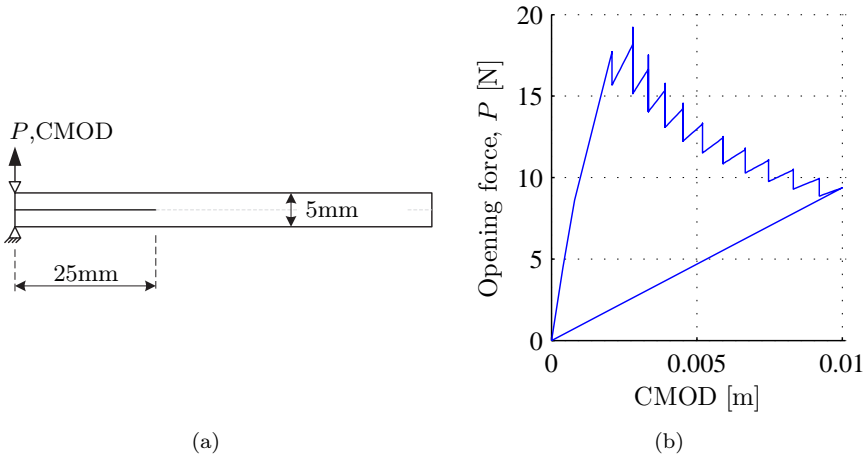
Figure 2.1: (a) a DCB model. CMOD is the crack mouth opening displacement and P is the opening force. (b) Finite element results of DCB response curves using 3.0mm large cohesive elements with 2×2 Newton-Cotes quadrature.

quadrature while for 30×30 Gauss-Legendre the error is only between 0.2% and 0.4%.

Furthermore, it is shown using DCB specimen models that there is a strong correlation between both the accuracy of the solution, the ability to obtain a converged solution and the magnitude of the integration error. By reducing the integration error in the damage process zone of the interface, more accurate results are obtained and larger elements can be utilized with less iterations, thereby decreasing the computational cost. Reducing the integration error increases the applicable size of cohesive elements and makes the model less sensitive to different settings like the magnitude of artificial damping and onset traction.

Since there is only a need for reducing the integration error in the damage process zone, an adaptive scheme can be applied such that only elements developing damage utilize a higher order integration. The extra computational cost associated to the increase in number of integration points in the damage zone is insignificant compared to the gain in computational efficiency obtained by increasing the element size. In a study of a three dimensional finite element model of a laminate containing a curved crack front the applicable element size was increased by a factor of 4 using 30×30 Gauss-Legendre quadrature instead of 2×2 Newton-Cotes quadrature. No significant change in the number of equilibrium iterations was observed and the response using 30×30 Gauss-Legendre quadrature with 4mm elements was closer to a converged response compared to the solution obtained with 2×2 Newton-Cotes quadrature and 1mm elements.

2.2 Paper B

Paper B with the title *Delamination under Fatigue Loads in Composite Laminates: A Review on the Observed Phenomenology and Computational Methods* [50] presents a review of the available experimental observations, the phenomenological models, and the computational simulation methods for the three phases of delamination (initiation, onset and propagation). First the available experimental work on characterization of the behavior of delamination is reviewed in order to clarify which capabilities are required from simulation methods and next currently available simulation methods are reviewed in regards to these capabilities.

The review of experimental observations covers the influence of different conditions, such as mixed-mode ratio, load ratio, mean load, and type of material, have on fatigue-driven delamination. The review of phenomenological models for onset and propagation clarifies that all available models are based on linear elastic fracture mechanics and can therefore be regarded as expansions of Paris' law [47]. Following the review of phenomenological models a review of the available simulation methods for initiation, no-growth, and propagation are given. The overall procedure and characteristics of the methods are described. This is done in a way that all common features of the methods are accentuated and the differences are discussed. The capabilities of the methods to reproduce experimental data or Paris' law under different conditions, e.g. mixed mode, are presented.

The amount of work dealing with delamination propagation exceeds by far the work on initiation and no-growth in regards to experimental observations, work on phenomenological models, and simulation methods.

Based on the review of the topic a list of recommendations for further research is given. One of the overall themes is to make the simulation methods suitable for structural design validation studies by increasing the accuracy and improving the predictive capabilities. Another overall theme is to extend the experimental data and simulation methods to more general loading conditions and three dimensional crack propagation as most current research is based on simple specimens such as the double cantilevered beam specimen consisting of a unidirectional laminate.

2.3 Paper C

Paper 3 with the title *A Simulation Method for High-Cycle Fatigue-Driven Delamination using a Cohesive Zone Model* [53] presents a new method for simulating fatigue-driven delamination under general mixed mode conditions. The method is based on a direct link between a mixed mode capable quasi-static cohesive model [34] and a Paris' law like model of the crack propagation rate of the type $da/dN = f(\Delta\mathcal{G}, \mathcal{G}_{\mathrm{mean}}, \phi)$. $\Delta\mathcal{G}$ and $\mathcal{G}_{\mathrm{mean}}$ describe the cyclic variation of the energy release rate $\mathcal{G}$ and ϕ is the mode mixity expressed in mode decomposed energy release rates, $\mathcal{G}_I$, $\mathcal{G}_{II}$ and $\mathcal{G}_{III}$. The method is

therefore capable of simulating both quasi-static and fatigue crack propagation without any parameter fitting. The link between the cohesive quasi-static law and the Paris' law like model is formulated such that the used Paris' law can be reproduced in finite element analyses with practically no error for any given structure or load.

The motivation for formulating this method came from the conclusions of the review in paper B, which displayed that the current methods for simulating fatigue driven delamination lack in accuracy and/or cannot be used as a predictive tool since parameter fitting is needed for the given structure being analysed in order to represent experimental results.

In order to keep the computational efficiency of the method reasonably for high-cycle fatigue, it has been based on the envelope load model approach. This means that only the envelope of the cyclic variation of the load on the structure is modelled and not the full cyclic variation, since this would have made the method computationally inefficient. The development of the damage variable of the cohesive interface is formulated as a damage rate with the following main dependencies:

$$\frac{dD}{dN} = f\left(\frac{\partial \lambda}{\partial a}, \frac{\partial \beta}{\partial a}, \frac{da}{dN}, ...\right) \tag{2.1}$$

where the rate of the interface opening displacement norm $\partial \lambda / \partial a$ and rate of the mode mixity $\partial \beta / \partial a$ with respect to crack extension are determined from the interface opening displacement field. The crack growth rate da/dN is determined using the mode decomposed J-integral [18, 31]. The remaining variables figuring in the expression for the damage rate, which have not been written out here, are derived from the quasi-static cohesive law.

The damage at a given cycle count is determined at discrete increments in cycles ΔN by integration of the damage rate. Like other fatigue crack propagation simulation methods the accuracy of this integration is affected by the size of the elements and the cycle increment. In order to balance out the integration error an adaptive cycle integration (ACI) scheme has been proposed which results in highly accurate results for coarse meshes and large cycle increments.

The method has been implemented as a zero thickness 8-noded interface element for Abaqus and as a spring element for a simple finite element model in Matlab. The method has been validated in simulations of mode I, mode II and mixed mode crack loading for both self-similar and non-self-similar crack propagation. The method produces highly accurate results compared to currently available methods and is capable of simulating general mixed mode non-self-similar crack growth problems.

Chapter 3

Contributions and impact

In this chapter the main contributions, the novelty and the impact of the work have been highlighted. The novelty and contributions of the work have been divided into knowledge produced and methods developments.

In the work of paper A the reasons for the problems associated with using large elements are described and a detailed description of the shape and change of the integrands of the element force vector and stiffness matrix during damage development is given. Furthermore, knowledge of how damping affects the response and behaves differently for large elements using different quadratures and the magnitude of integration error is established. The paper provides a method to increase the efficiency and accuracy by simply reducing the integration error for the elements located in the damage process zone only. This has been demonstrated to provide the most significant improvements for three dimensional applications where the need for increased efficiency is the most critical.

The work of paper B provides a review on the observed phenomenology and computational methods for delamination under fatigue loads in composite laminates. The main contributions of this work are structuring and categorizing the knowledge within the research field and identifying the unsolved problems and areas where research is missing. The common features of the overall approach of the methods are described and serves as an introduction to the fundamentals of the topic of simulation methods for fatigue driven delaminations. Special attention is given to comment on the validation exercises of each of the reviewed methods in order to clarify for the reader what are the capabilities of currently available methods. Furthermore, a unified nomenclature for the simulation methods has been proposed which will support the reader of current and future work in the research field.

The main contribution of the work presented in paper C is focused on method development in the form of a novel fatigue method capable of simulating both quasi-static and fatigue driven delamination. The method produces significantly more accurately results for delaminations loaded in any given mode

mixity than current available methods. As a part of the method a link between the propagation of a sharp crack (in the classical fracture mechanics sense) and the local opening of a cohesive interface has been established which is expected to be of such general value that it can be used in other works where this link is needed. For the integration of the damage rate a novel predictor-corrector approach has been developed which the authors expect could be used to increase the size of applicable element and cycle increment with most of the other methods based on the envelope load model approach described in paper B. Comparison with existing methods have been made for self-similar delamination propagation (constant mode mixity and energy release rate) where it is shown that the proposed method is significantly more accurate than currently available methods. Furthermore, the capabilities in regards to simulating non-self-similar delamination propagation (gradually changing mode mixity and blockwise or gradually changing energy release rate) have been demonstrated with very high accuracy. Paper C also provides guidelines for choosing the element size and cycle increment based on sensitivity studies.

The impact of the contributions of the Ph.D. work is expected to be equally divided between the research community and the engineers working in the industry. The research community can benefit from the knowledge generated by the analyses of paper A which can benefit in the development of improved solutions to the problem of coarse mesh. Both new and experienced researchers can benefit from the review of the observed phenomenology and computational methods for delamination under fatigue loads paper B provides as well as find inspiration in the suggestions for further research for formulation of new research goals. The methods developed in paper C can be used as tools for the development of other methods where e.g. the link between the advance of a discrete crack and opening of a cohesive interface is needed or where application of the adaptive cycle integration (ACI) scheme can be used to obtain more accurate solutions. The engineers in the industry can benefit from all three papers. Paper A and C provide means to obtain more accurate results and increased computational efficiency in quasi-static and fatigue analyses. Paper B provides a overview and insight in the topic of fatigue-driven delamination which can aid in the effects to consider and models and methods to use for simulation.

Chapter 4

Perspectives and future work

During the work of the Ph.D. project, progress has been made and new problems and unsolved questions have been raised. During the work the problems yet not solved were revealed which turns into the following suggestions for further work. With regard to fatigue driven delaminations paper B provides a more elaborated list of suggestions for further research which is not repeated here.

- Investigate if further reduction of the computational cost can be obtained by combining a reduced integration error, as shown in paper A, in combination with enriched/higher order elements.

- The analysis of paper A showed how damping of the damage parameter does not work as intended and that it is sensitive to the integration scheme. Thus, a better damping formulation on field variables such as the rate of energy dissipation of the cohesive interface should be further looked into in order to increase the computational efficiency and accuracy of delamination simulations.

- Extend the J-integral formulation used in paper C for three dimensional cohesive interfaces in order to enable the simulation of 3D crack growth using the method provided in Paper C.

- Extend the current capabilities of modelling cyclic loading to general or more real world representative loading spectra.

- Extend cohesive law and damage formulation to three dimensional analyses where all three crack opening modes are treated.

- Provide a well-defined set of benchmark examples for fatigue driven three dimensional crack growth problems to test simulation methods. This include experimental data at coupon level to be used for model calibration and subcomponent/substructure data for model validation.

References

[1] US Department of Energy. Annual Energy Outlook 2013, DOE/EIA-0383. *Technical Report*, U.S. Energy Information Administration, Washington DC 2012.

[2] Leong M, Overgaard LCT, Thomsen OT, Lund E, Daniel IM. Investigation of failure mechanisms in GFRP sandwich structures with face sheet wrinkle defects used for wind turbine blades. *Composite Structures* 2012; **94**(2):768–778.

[3] Griffith AA. The phenomena of rupture and flow in solids. *Philosophical Transactions of the Royal Society of London. Series A, Containing Papers of a Mathematical or Physical Character* 1921; **221**:163–198.

[4] Lawn BR. *Fracture of Brittle Solids*. Second edn., Cambridge University Press: New York, NY, 1993.

[5] Barenblatt GI. Concerning equilibrium cracks forming during brittle fracture: the stability of isolated cracks. *Journal of Applied Mathematics and Mechanics* 1959; **23**:622–636.

[6] Hashemi S, Kinloch AJ, Williams JG. The Analysis of Interlaminar Fracture in Uniaxial Fibre-Polymer Composites. *Proceedings of the Royal Society of London. A. Mathematical and Physical Sciences* 1990; **427**(1872):173–199.

[7] Albertsen H, Ivens J, Peters P, Wevers M, Verpoest I. Interlaminar fracture toughness of CFRP influenced by fibre surface treatment: Part 1. Experimental results. *Composites Science and Technology* 1995; **54**(2):133–145.

[8] Spearing SM, Evans AG. The role of fiber bridging in the delamination resistance of fiber-reinforced composites. *Acta Metallurgica et Materialia* 1992; **40**(9):2191–2199.

[9] Sørensen BF. Cohesive laws for assessment of materials failure: Theory, experimental methods and application 2010. Doctor Technices Thesis, 2010.

[10] Xia ZC, Hutchinson JW. Mode II fracture toughness of a brittle adhesive layer. *International Journal of Solids and Structures* 1994; **31**(8):1133–1148.

[11] Dugdale DS. Yielding of steel sheets containing slits. *Journal of the Mechanics and Physics of Solids* 1960; **8**(2):100–104.

[12] Hillerborg A, Modéer M, Petersson PE. Analysis of crack formation and crack growth in concrete by means of fracture mechanics and finite elements. *Cement and Concrete Research* 1976; **6**(6):773–781.

[13] Van Mier JGM. Mode I fracture of concrete: discontinuous crack growth and crack interface grain bridging. *Cement and Concrete Research* 1991; **21**(1):1–15.

[14] Camacho GT, Ortiz M. Computational modelling of impact damage in brittle materials. *International Journal of Solids and Structures* 1996; **33**(20-22):2899–2938.

31

[15] Tvergaard V, Hutchinson JW. The relation between crack growth resistance and fracture process parameters in elastic-plastic solids. *Journal of the Mechanics and Physics of Solids* 1992; **40**(6):1377–1397.

[16] Hansen AL, Lund E. Simulation of delamination including fiber bridging using cohesive zone models. *ECCOMAS Thematic Conference on Mechanical Response of Composites*, Camanho PP (ed.), ECCOMAS, 2007.

[17] Ortiz M, Pandolfi A. Finite-deformation irreversible cohesive elements for three-dimensional crack-propagation analysis. *International Journal for Numerical Methods in Engineering* 1999; **44**(9):1267–1282.

[18] Rice JR. A path independent integral and the approximate analysis of stress concentration by notches and cracks. *Journal of Applied Mechanics* 1968; **35**(2):379–386.

[19] Sørensen BF, Kirkegaard P. Determination of mixed mode cohesive laws. *Engineering Fracture Mechanics* 2006; **73**(17):2642–2661.

[20] Lindgaard E, Bak BLV, Andreasen JA, Sørensen BF, Jensen HM, Turon A, Hansen AL. Ph.d. course on Fracture Mechanics for Laminated Composite Structures. *Aalborg University, Department of Mechanical and Manufacturing Engineering* 2012; .

[21] Needleman A. A continuum model for void nucleation by inclusion debonding. *Journal of Applied Mechanics* 1987; **54**(3):525–531.

[22] Needleman A. An analysis of tensile decohesion along an interface. *Journal of the Mechanics and Physics of Solids* 1990; **38**(3):289–324.

[23] Kim YR. Cohesive zone model to predict fracture in bituminous materials and asphaltic pavements: state-of-the-art review. *International Journal of Pavement Engineering* 2011; **12**(4):343–356.

[24] Hui CY, Ruina A, Long R, Jagota A. Cohesive zone models and fracture. *The Journal of Adhesion* 2011; **87**(1):1–52.

[25] Turon A, Davila C, Camanho P, Costa J. An engineering solution for mesh size effects in the simulation of delamination using cohesive zone models. *Engineering Fracture Mechanics* 2007; **74**(10):1665–1682.

[26] Planas J, Elices M. Asymptotic analysis of a cohesive crack. 2: Influence of the softening curve. *International Journal of Fracture* 1993; **64**:221–237.

[27] Alfano G. On the influence of the shape of the interface law on the application of cohesive-zone models. *Composites Science and Technology* 2006; **66**(6):723–730.

[28] Williams ML. The stresses around a fault or crack in dissimilar media. *Bulletin of the Seismological Society of America* 1959; **49**(2):199–204.

[29] Benzeggagh ML, Kenane M. Measurement of mixed-mode delamination fracture toughness of unidirectional glass/epoxy composites with mixed-mode bending apparatus. *Composites Science and Technology* 1996; **56**(4):439–449.

[30] Blanco N, Gamstedt EK, Asp LE, Costa J. Mixed-mode delamination growth in carbon-fibre composite laminates under cyclic loading. *International Journal of Solids and Structures* 2004; **41**(15):4219–4235.

[31] Huber O, Nickel J, Kuhn G. On the decomposition of the J-integral for 3D crack problems. *International Journal of Fracture* 1993; **64**(4):339–348.

[32] Rigby RH, Aliabadi MH. Decomposition of the mixed-mode J-integral –revisited. *International Journal of Solids and Structures* 1998; **35**(17):2073–2099.

[33] Camanho PP, Davila CG, de Moura MF. Numerical simulation of mixed-mode progressive delamination in composite materials. *Journal of Composite Materials* 2003; **37**(16):1415–1438.

[34] Turon A, Camanho PP, Costa J, Dávila CG. A damage model for the simulation of delamination in advanced composites under variable-mode loading. *Mechanics of Materials* 2006; **38**(11):1072–1089.

[35] Turon A, Camanho PP, Costa J, Renart J. Accurate simulation of delamination growth under mixed-mode loading using cohesive elements: Definition of interlaminar strengths and elastic stiffness. *Composite Structures* 2010; **92**(8):1857–1864.

[36] Sarrado C, Turon A, Renart J, Urresti I. Assessment of energy dissipation during mixed-mode delamination growth using cohesive zone models. *Composites Part A: Applied Science and Manufacturing* 2012; **43**(11):2128–2136.

[37] Högberg JL, Sørensen BF, Stigh U. Constitutive behaviour of mixed mode loaded adhesive layer. *International Journal of Solids and Structures* 2007; **44**(25-26):8335–8354.

[38] Park K, Paulino GH. Cohesive zone models: a critical review of traction-separation relationships across fracture surfaces. *Applied Mechanics Reviews* 2011; **64**(6):060 802.

[39] Park K, Paulino GH, Roesler JR. A unified potential-based cohesive model of mixed-mode fracture. *Journal of the Mechanics and Physics of Solids* 2009; **57**(6):891–908.

[40] Goutianos S, Sørensen BF. Path dependence of truss-like mixed mode cohesive laws. *Engineering Fracture Mechanics* 2012; **91**:117–132.

[41] Simo JC, Ju JW. Strain- and stress-based continuum damage models – I. Formulation. *International Journal of Solids and Structures* 1987; **23**(7):821–840.

[42] Goyal VK. Analytical modeling of the mechanics of nucleation and growth of cracks. PhD Thesis, Faculty of Virginia Polytechnic Institute and State University, USA 2002.

[43] Sutherland HJ. On the fatigue analysis of wind turbines. *Technical Report*, Sandia National Laboratories, New Mexico 1999.

[44] Miner MA. Cumulative damage in fatigue. *Journal of Applied Mechanics* 1945; **12**(3):159–164.

[45] Palmgren A. Die Lebensdauer von Kugellagern. *Zeitschrift des Vereines Deutcher Ingenieure* 1924; **68**(14):339–341.

[46] ASTM E1049-85(2011)e1, Standard practices for cycle counting in fatigue analysis. *Technical Report*, ASTM International, www.astm.org 2011.

[47] Paris PC, Gomez MP, Anderson WE. A rational analytic theory of fatigue. *The trend in engineering* 1961; **13**(1):9–14.

[48] Peerlings RHJ, Brekelmans WAM, de Borst R, Geers MGD. Gradient-enhanced damage modelling of high-cycle fatigue. *International Journal for Numerical Methods in Engineering* 2000; **49**(12):1547–1569.

[49] Robinson P, Galvanetto U, Tumino D, Bellucci G, Violeau D. Numerical simulation of fatigue-driven delamination using interface elements. *International Journal for Numerical Methods in Engineering* 2005; **63**(13):1824–1848.

[50] Bak BLV, Sarrado C, Turon A, Costa J. Delamination Under Fatigue Loads in Composite Laminates: A Review on the Observed Phenomenology and Computational Methods. *Applied Mechanics Reviews* 2014; **66**(6):1–24.

[51] Overgaard LCT, Lund E. Structural collapse of a wind turbine blade. Part B: Progressive interlaminar failure models. *Composites Part A: Applied Science and Manufacturing* 2010; **41**(2):271–283.

[52] Bak BLV, Lindgaard E, Lund E. Analysis of the integration of cohesive elements in regard to utilization of coarse mesh in laminated composite materials. *International Journal for Numerical Methods in Engineering* 2014; **99**(8):566–586.

[53] Bak BLV, Turon A, Lindgaard E, Lund E. A Simulation Method for High-Cycle Fatigue-Driven Delamination using a Cohesive Zone Model. *Submitted to: International Journal for Numerical Methods in Engineering* 2014; .

SUMMARY

The overall purpose of this Ph.D. project has been to develop a framework of methods for progressive delamination modeling and simulation of composite laminates in large scale structures under both quasi-static and fatigue loading. The first part of the thesis is an introduction to the project and provides a short introduction to selected basic topics of the theoretical background of the work presented in the papers.

The second part of the thesis consists of three refereed journal papers.

Paper A is concerned with computational efficiency and the ability to converge to a solution for large cohesive elements applied in delamination analyses.

Paper B presents a review of the available experimental observations, the phenomenological models and the computational simulation methods for the three phases of fatigue-driven delamination (initiation, onset and propagation).

Paper C presents a new method for simulating fatigue-driven delamination under general mixed mode conditions. The experimental crack growth rate can be reproduced in finite element analyses with practically no error for any given structure and load.